

Supporting Information

Facile One-Step Room-Temperature Synthesis of Pt₃Ni Nanoparticle

Networks with Improved Electro-catalytic Properties

You Xu, Shuangxia Hou, Yang Liu, Yue Zhang, Huan Wang and Bin Zhang*

Department of Chemistry, School of Science, Tianjin University, Tianjin 300072, P. R. China

E-Mail: bzhang@tju.edu.cn

S1. Experimental Section

1.1 Chemicals: All chemicals were of analytical grade and were used as received without further purification. Aqueous solutions were prepared by using Milli-Q water.

1.2 Synthesis of Pt₃Ni Nanoparticle Networks (Pt₃Ni NN): In a typical preparation of the Pt₃Ni alloy, a mixture aqueous solution of H₂PtCl₆ (3.75 mL, 20mM) and NiCl₂ (1.25 mL, 20mM) was added to cetyltrimethyl ammonium bromide (CTAB, 5 mL, 40 mM) solution (the solvent is chloroform). 10 mL of Milli-Q water and 30 mL of ethylene glycol was added to the above mixture solution under constant strong stirring and kept stirring for 30 min. Then, 5 mL freshly prepared 1.0M NaBH₄ aqueous solution was quickly injected into the above solution and kept stirring at a speed of 1500 rpm for 20 min. The black as-prepared precipitates were collected and washed several times with distilled water and ethanol, respectively.

1.3 Synthesis of Pt Nanoparticle Networks (Pt NN): For the synthesis of Pt NN, the experimental parameters are the same to the procedure of the preparation of Pt₃Ni NN, except that the addition of NiCl₂ (1.25 mL, 20 mM) is replaced by H₂PtCl₆ (1.25 mL 20 mM).

1.4 Synthesis of Pd Nanoparticle Networks (Pd NN): The procedure for the preparation of Pd NN is the same to that described in Section 1.3 except that the 5mL H₂PdCl₄ (20 mM) was added to the initial reacting mixture.

1.5 Synthesis of Au Nanoparticle Networks (Au NN): The procedure for the preparation of Au NN is the same to that described in Section 1.3 except that the 5mL HAuCl₄ (20 mM) was added to the initial reacting mixture.

1.6 Synthesis of Pt-Co Nanoparticle Networks (Pt-Co NN): The procedure for the

preparation of Pt-Co NN is the same to that described in Section 1.3 except that the 3.75 mL H₂PtCl₆ (20 mM) and 1.25 mL CoCl₂ (20 mM) was added to the initial reacting mixture.

1.7 Synthesis of PtNi, Pt₂Ni and Pt₄Ni NN: The procedure for the preparation of Pt-Ni NN with different composition is the same to that described in Section 1.2 except that different molar ratio of metal precursors was added to the initial reacting mixture. Detailedly, for PtNi NN, H₂PtCl₆ (2.5mL, 20mM) and NiCl₂ (2.5mL, 20mM) was added; for Pt₂Ni NN, 3.33mL of 20mM H₂PtCl₆ and 1.67mL of 20mM NiCl₂ was added; for Pt₄Ni NN, 4mL of 20mM H₂PtCl₆ and 1mL of 20mM NiCl₂ was adopted.

1.8 Electrochemical Measurements:

All electrochemical measurements were performed using an electrochemical workstation (CHI 660, CH Instruments, Austin, TX). A Pt wire was served as counter electrode, an Ag/AgCl electrode saturated with KCl was utilized as reference electrode (separated by a electrolyte bridge). In oxygen reduction reaction test, a glassy carbon rotating disk electrode (ATA-1B, Jiangfen Electroanalytical Instruments, Jiangsu, diameter: 3 mm; area: 0.071 cm²) was used as working electrode. In methanol and formic acid oxidation measurements, the working electrode is a glassy carbon electrode. All potentials, if not specified, are normalized to the Reversible Hydrogen Electrode (RHE) in this work. The catalysts were assembled on the working electrode by drop-coating to obtain the working electrode. In a typical preparing process of working electrode, 2 mg of Pt₃Ni catalyst was dispersed in 2 mL of a mixture solvent (the volume ratio of H₂O: isopropanol: 5% Nafion is 4:1:0.025), and the mixture was sonicated for 5 min to get a dispersed suspension. Then 2μL of the suspension was dropped onto the RDE and dried in flowing argon. So the Pt loading on the working electrode was calculated to be 25.3μg_{pt}/cm². The preparing processes for Pt NN and commercial Pt/C working electrodes were similar to that of Pt₃Ni electrode. The corresponding Pt loading for Pt NN and Pt/C were the same to that of Pt₃Ni NN (25.3 μg_{pt}/cm²). In order to produce a clean electrode surface, the working electrode was cleaned in 0.5M H₂SO₄ by potential cycling between +0.05 and +1.0V at 100 mV/s until stable voltammogram was obtained. Specifically, cyclic voltammetrys (CVs) were performed in a deoxygenated 0.5M H₂SO₄ solution at a scan rate of 50 mV/s.

For oxygen reduction reaction, the measurements were performed in 0.5 M O₂-saturated

H₂SO₄ solutions using the glassy carbon RDE at a rotation rate of 1,600 rpm and a sweep rate of 5 mV/s.

For methanol oxidation and formic acid oxidation, CVs were performed in 0.5 M H₂SO₄+0.5 M methanol and 0.5 M H₂SO₄ + 0.5 M formic acid at a scan rate of 50 mV/s, respectively.

Chronoamperometry was test in 0.5 M H₂SO₄ + 0.5 M methanol at a given potential of 0.75V for methanol oxidation and 0.5 M H₂SO₄ + 0.5 M formic acid at 0.55V for formic acid oxidation.

1.9 Characterization: The scanning electron microscopy (SEM) images and Energy-dispersive X-ray spectroscopic (EDX) analysis were taken with a Hitachi S-4800 scanning electron microscope (SEM, 5 kV) equipped with the Thermo Scientific energy-dispersion X-ray fluorescence analyzer. Transmission electron microscopy (TEM), and high-resolution transmission electron microscopy (HRTEM) images were obtained with JEOL-2100F system. Specimens for TEM and HRTEM measurements were prepared via dropcasting a droplet of ethanol suspension onto a copper grid, coated with a thin layer of amorphous carbon film, and allowed to dry in the air. Inductively coupled plasma(ICP) analysis was conducted in a VISTA-MPX inductive coupling plasma emission spectrograph .The X-ray diffraction patterns (XRD) of the products were recorded with Bruker D8 Focus Diffraction System using a Cu K α source ($\lambda= 0.154178$ nm).

S2 Figures

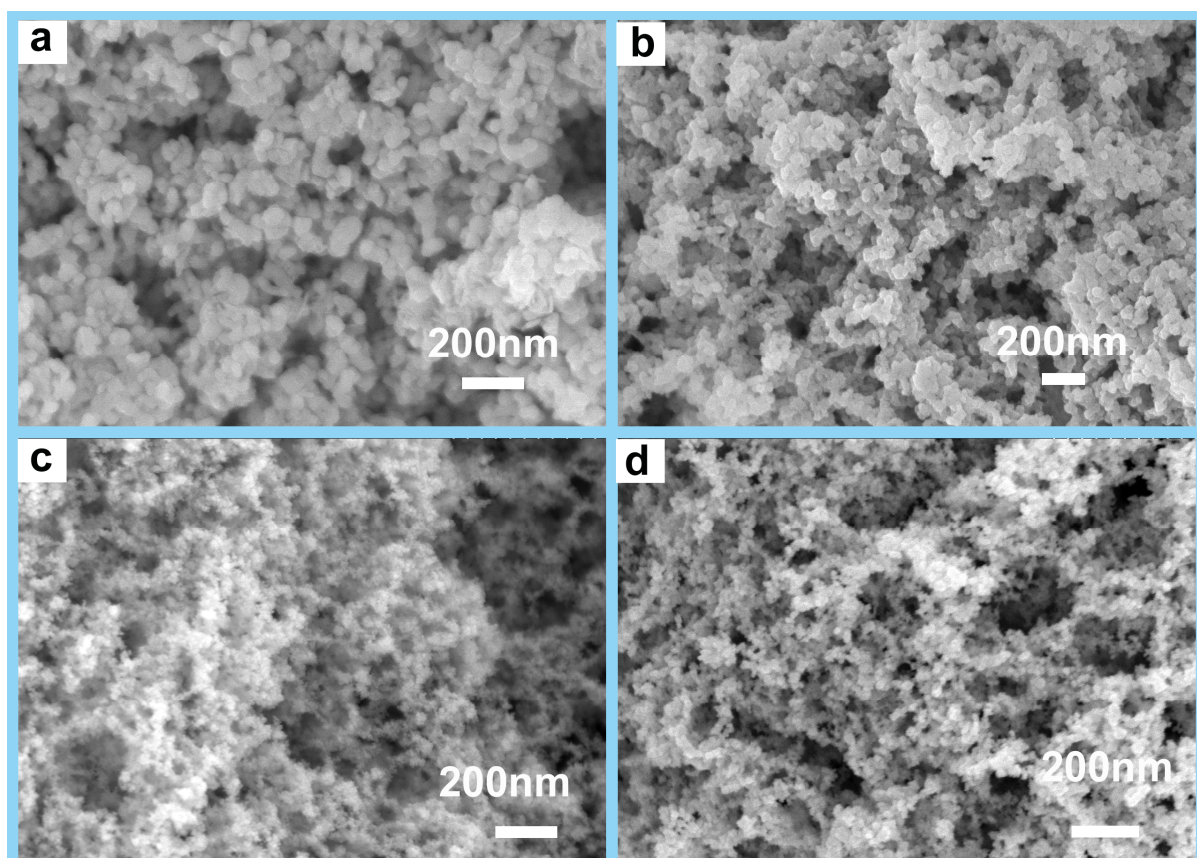


Figure S1. SEM images of Pt₃Ni alloy prepared by adding different amount of EG: 0 mL (a); 10 mL (b); 30 mL (c); 40 mL (d). The decrease of EG was compensated with the same volume of Milli-Q water. It was found that the presence of EG can influence the formation of the network-like structure and the size of the nanoparticles.

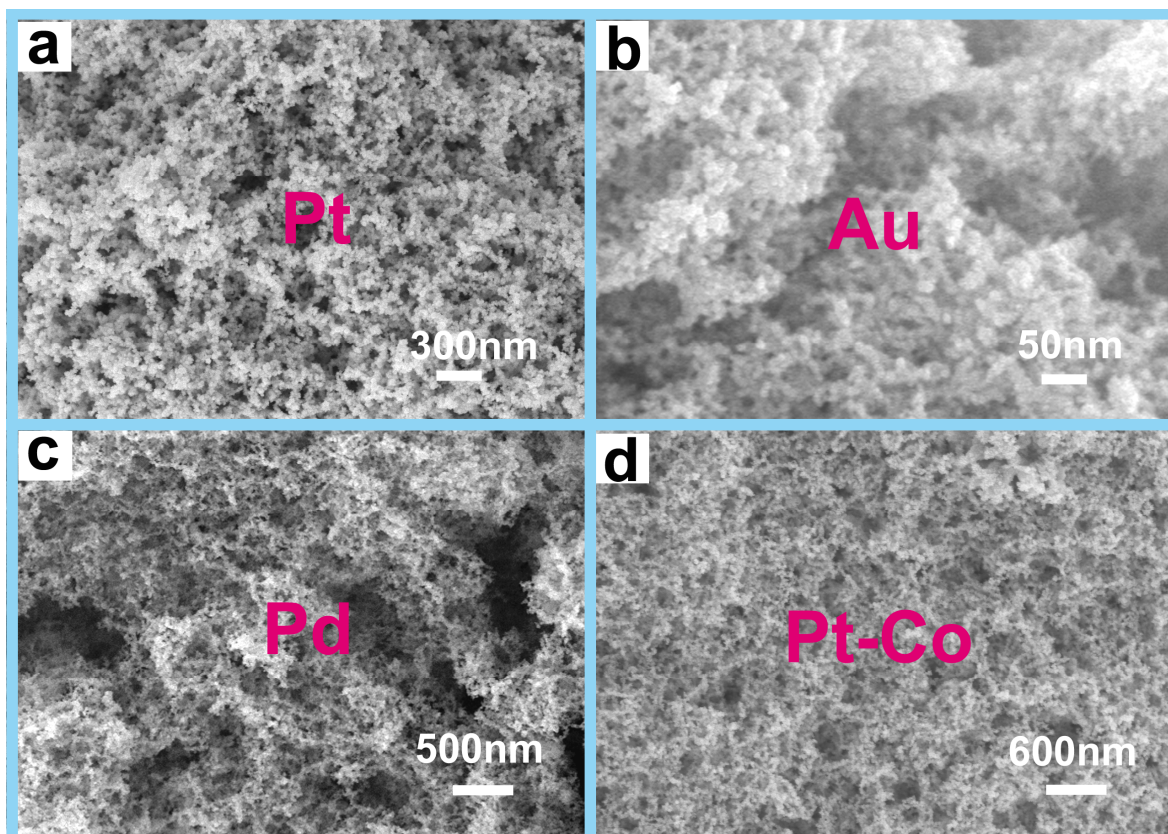


Figure S2. (a-d) SEM images of different metals or alloy nanoparticle networks: Pt NN(a), Au NN(b), Pd NN(c), Pt-Co NN(d). It was shown that our approach can be extended to prepare pure noble metals(Pt, Au, Pd) and some other Pt-based alloys (e.g. Pt-Co) networks composed of sub-10 nm nanoparticles.

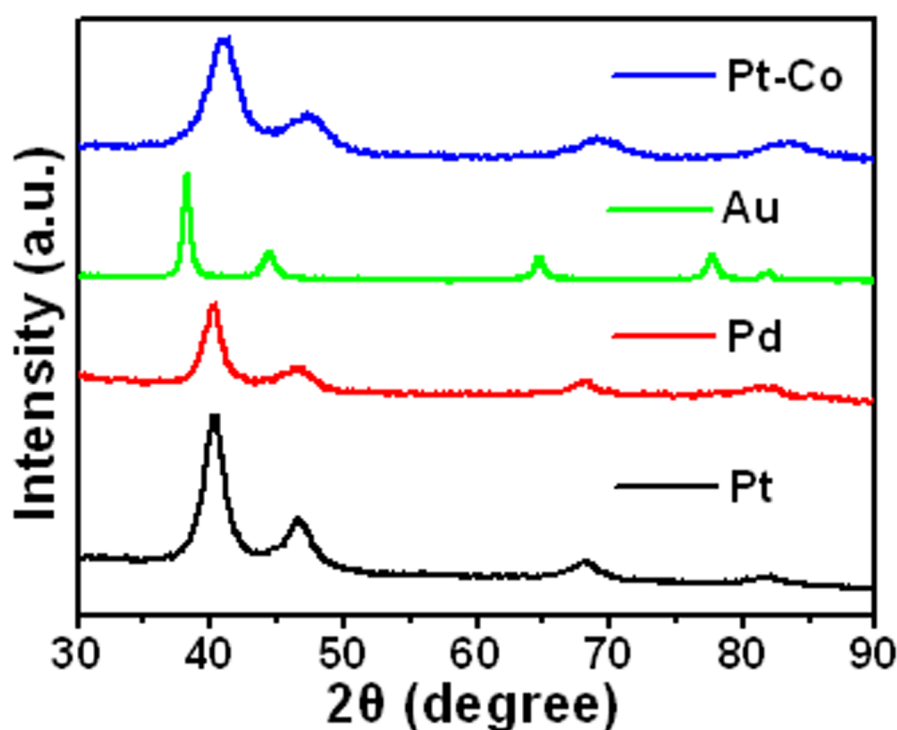


Figure S3. XRD patterns of Pt NN, Au NN, Pd NN, and PtCoNN.

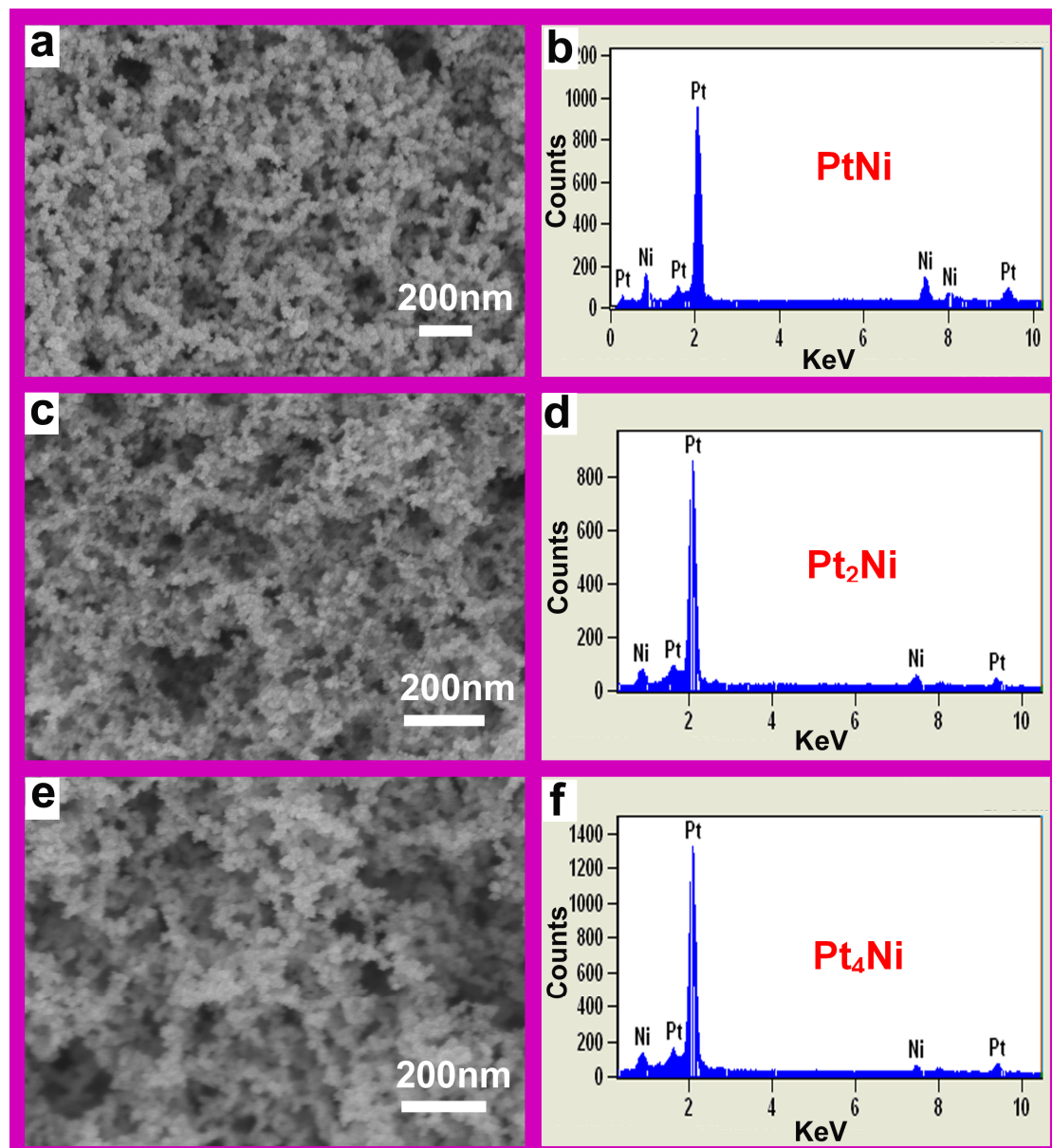


Figure S4. SEM images (a,c,e) and EDX spectrums (b,d,f) of Pt-Ni alloy NN with different composition: PtNi NN (a,b); Pt₂Ni NN(c,d); Pt₄Ni NN(e,f). It was demonstrated that the composition of Pt-Ni alloy NN can be modulated by changing the molar ratio of metal precursors in our synthesis approach.

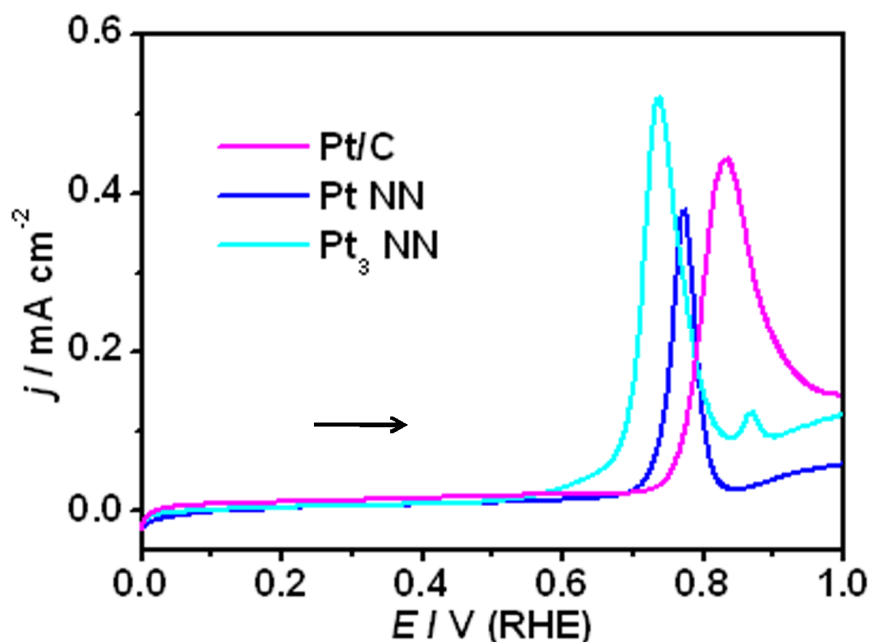


Figure S5. Cyclic voltammograms of Pt_3Ni NN, Pt NN and Pt/C NN electrodes in 0.5 M H_2SO_4 after immersion in CO saturated 0.1 M H_2SO_4 for 5 min at open circuit potential. Scan rate: 50 mV/s. The strong stripping peak of CO on Pt_3Ni NN electrode is centered at 0.73V, which is about 35 mV and 95 mV more negative than those on Pt NN and Pt/C, respectively. This suggests that CO can be more easily oxidized on a Pt_3Ni alloy NN, indicating that the bifunctional mechanism may be used to explain the improved electrocatalytic activities of Pt_3Ni NN. As for the very weak peaks of CO stripping at ca. 0.87 V, its origin is still unclear and should be further studied.

S3. Co-reduction mechanism of Pt-Ni NN.

To further explore the composition of the NN, the influence of standard reduction potentials (SRP) is studied. It is known that the SRP for Ni^{2+} and $[\text{PtCl}_6]^{2-}$ are -0.28 V and +0.68 V versus normal hydrogen electrode (NHE), respectively. Thermodynamically, different metals prefer to nucleate and grow separately in the wet-chemical synthetic process due to their different SRPs. The more positive reduction potential gives the $[\text{PtCl}_6]^{2-}$ ions a much higher tendency to be reduced before Ni^{2+} when they coexist, preferring to form the Pt@Ni core-shell structure or hierarchical structure which may lead to phase separation. In our synthesis system, several key factors ensure the simultaneous appearance of Pt and Ni atoms at both nucleation and growth stages. On one hand, the existence of CTAB which may form Pt complex with $[\text{PtCl}_6]^{2-}$ may influence redox potentials of $[\text{PtCl}_6]^{2-}$. On the other hand, the strong reducing agent NaBH_4 helps to reduce simultaneously all metal precursors at proper rates.(Z. Peng and H. Yang, Nano Today, 2009, 4, 143–164.) In addition, $[\text{PtCl}_6]^{2-}$ reduction to Pt requires two steps ($[\text{PtCl}_6]^{2-}$ - $[\text{PtCl}_4]^{2-}$ -Pt).(L. Liu and E. Pippel, Angew. Chem., Int. Ed., 2011, 50, 2729–2733.) These conditions effectively promote the co-reduction and facilitate the generation of alloy NN. On the base of co-reduction in our synthesis system, it is reasonable to expect that the composition of bimetallic alloy NN can be modulated by changing some reaction conditions (Z. Peng and H. Yang, Nano Today, 2009, 4, 143–164; R. Riccardo, J. Jellinek and R. L. Johnston, Chem. Rev., 2008, 108, 845–910.) .